Functional and Structural Roles of Critical Amino Acids within the"N", "P", and "A" Domains of the Ca^{2+} ATPase (SERCA) Headpiece†

Hailun Ma,‡ David Lewis,‡ Cheng Xu,‡ Giuseppe Inesi,*,‡ and Chikashi Toyoshima§

Department of Biochemistry and Molecular Biology, University of Maryland School of Medicine, Baltimore, Maryland 21201, and Institute of Molecular and Cellular Biosciences, The University of Tokyo, Bunkyo-ku, Tokyo 113-0032, Japan

Received February 22, 2005; Revised Manuscript Received April 8, 2005

ABSTRACT: Twenty five amino acids within the "N", "P", and "A" domains of the Ca^{2+} ATPase (SERCA1) headpiece were subjected to site directed mutagenesis, taking advantage of a high yield expression system. Functional and conformational effects of mutations were interpreted systematically in the light of the high resolution WT structure, defining direct involvement in catalysis as well as in stabilization of various positions acquired by each domain upon substrate binding and utilization. Amino acids involved in binding of ATP (such as Phe487 and Arg560 in the N domain) or phosphate (such as Asp351, Thr625, Lys684, and Thr353 in the P domain) were characterized with respect to their binding mechanism. Further identified were "positional" roles of several amino acids that stabilize neighboring residues for optimal binding of substrate or Mg^{2+}, or interface between headpiece domains as they change their relative positions in the course of the catalytic cycle. These include cross-linking of the "N" and "P" domains (e.g., Arg560/Asp627 salt bridge to stabilize domain approximation by ATP binding), and stabilization of the "A", "N", and activated "P" domains in arrangements differing from the ground E2 state and driven by catalytic events. This stabilization is produced through hydrogen bonds at domain interfaces, which vary depending on the intermediate state (e.g., Glu486/T171 in E1P and E2P, as opposed to Glu486/H190 in E2). We demonstrate that specific arrangements of the headpiece domains shown in crystal structures are, in fact, required to trigger displacement of transmembrane segments during the enzyme cycle in solution, allowing long range linkage of catalytic and Ca^{2+} binding functions.

The sarco-endoplasmic reticulum Ca^{2+} ATPase (SERCA) is an integral membrane bound protein that sustains active transport of Ca^{2+}, coupled to utilization of ATP. The catalytic and transport cycle includes a number of sequential steps, beginning with activation of the enzyme ground state (E2) by high affinity binding of 2 Ca^{2+} ($E1{\cdot}2Ca^{2+}$), followed by utilization of ATP to form a phosphorylated enzyme intermediate ($ADP{\cdot}E1P{\cdot}2Ca^{2+}$). Dissociation of ADP and isomerization of phosphoenzyme from $E1P{\cdot}2Ca^{2+}$ to $E2P{\cdot}2Ca^{2+}$ then promote vectorial dissociation of the bound Ca^{2+}. Finally, the cycle is completed by hydrolytic cleavage of P_i from E2P (*1*).

The ATPase sequence includes 994 amino acids (*2*) arranged in 10 α-helical segments within the transmembrane region, and three headpiece domains ("N", "P", and "A") protruding from the cytosolic surface of the membrane. Separation, rotation, and gathering of the three cytosolic domains, as well as displacement and bending of the transmembrane segments, occur in concomitance with the sequential steps of the ATPase cycle. These changes were revealed by structural analysis of E2(TG) (PBD accession number 1IWO), $E1{\cdot}2Ca^{2+}$ (ISO4), E1·AMP-PCP[1] (1VFP; 1T5S), $E1{\cdot}AlF_x{\cdot}ADP$ (1WPE), and $E2{\cdot}MgF_4^{2-}$ (1WPG) crystals (*3*−*7*), in which AMP-PCP is an unhydrolyzable analogue of ATP, whereas AlF_x and MgF_4^{2-} are stable analogues of phosphates. Conformational heterogeneity has been observed in solution as well, in agreement with the crystallographic definition of different states (*8*).

Detailed characterization of the Ca^{2+} binding and occlusion mechanism within the transmembrane region was provided by mutational (*9*−*13*) and crystallographic analysis (*3*, *5*). Furthermore, a significant level of information has been obtained on the ATPase headpiece, identifying residues involved in nucleotide binding ("N" domain), phosphoenzyme formation ("P" domain), and various catalytic reactions (*3*, *14*−*22*). We are here reporting an extensive mutational analysis of the headpiece domain, interpreted in the light of high resolution WT structure to examine in detail the catalytic and/or positional roles of amino acids in the "N", "P", and "A" domains (Figure 1). Taking advantage of a high yield recombinant ATPase expression system, we examine steady state ATPase activity and phosphorylation by ATP or P_i, as well as the protection effect of AMP-PCP and AlF_x against proteinase K digestion in the presence of Ca^{2+}. The primary

† This work was supported by the NHLB, National Institutes of Health Grant RO1 HL69830.

* Author to whom correspondence should be addressed. E-mail: ginesi@umaryland.edu. Tel: 410-706-3220. Fax: 410-706-8297.

‡ University of Maryland School of Medicine.

§ The University of Tokyo.

[1] Abbreviations: MOPS, 3-[*N*-morpholino]propanesulfonic acid; MES, 2-[*N*-morpholino]ethanesulfonic acid; EGTA, ethylene glycol bis-(β-aminoethyl ether)-*N*,*N*,*N*′,*N*′-tetraacetic acid; BSA, bovine serum albumin; AMP-PCP, β,γ-methyleneadenosine 5′-triphosphate; Tris, tris-(hydroxymethyl)aminomethane; WT, wild type.

10.1021/bi050332m CCC: $30.25
Published on Web 05/11/2005

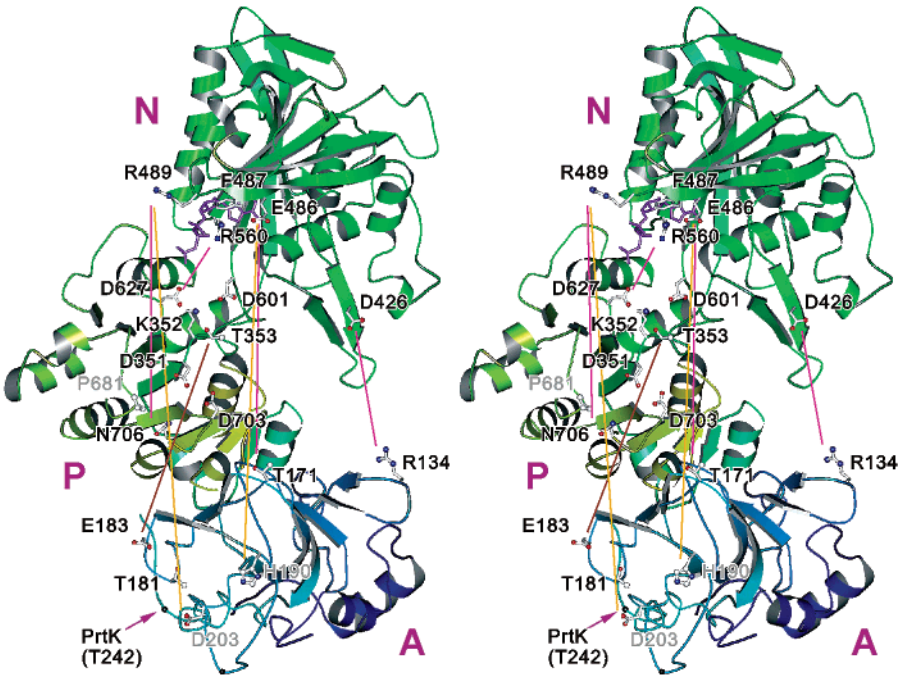

FIGURE 1: View (stereo) from the top of the ATPase headpiece in the E1·2Ca^{2+} crystal structure (PDB accession code 1SU4). Colors change gradually from the N-terminus (blue) to the C-terminus (red); thus, "A", "P", and "N" domains appear in different colors. The residues in the A and N domains subjected to mutational analysis are shown in ball-and-stick. Some of the mutated residues in the P domain are not shown. Different lines represent interdomain interactions in different conformational states (pink, E1·ATP-E1·P; orange, E2P; brown, E2). Labels in gray refer to the residues that were not mutated but are likely to be involved in interdomain interactions. ATP in the extended conformation that was observed with E1·AMP-PCP crystals is shown with purple sticks. Prepared with Molscript (*39*).

digestion site is located at Thr242 (Figure 1), on the loop connecting the M3 transmembrane helix and the A domain. This protection is realized apparently by tilting of the A domain and stressing of the M3-A domain. From the crystallographic study (*5*), it is clear that the P-domain distortion is necessary for the tilting but ambiguous to what extent the N domain contributes. Since Ca^{2+}-ATPase is a member of the haloacid dehalogenase superfamily (*23*), high resolution structures of phosphoserine phosphatase (*24*), another member of the same superfamily, are also consulted for the residues in the P domain.

MATERIALS AND METHODS

Recombinant ATPase was obtained by exogenous gene expression in COS-1 cells infected with adenovirus vectors carrying chicken WT or mutated SERCA1 cDNA (*25*). Adenovirus construction, site directed mutagenesis, COS-1 cell culture methods, and preparation of microsomal fractions were previously described (*26*). Protein concentration was measured using bicinchoninic acid with the biuret reaction (Pierce).

ATPase hydrolytic activity was measured in the presence of 20 mM MOPS, pH 7.0, 80 mM KCl, 3 mM $MgCl_2$, 0.1 mM $CaCl_2$, 5 mM sodium azide, 3 μM ionophore A23187, and 10 μg of microsomal protein/mL. The reaction was started by adding 3 mM ATP, and samples were collected at serial times for P_i determination by the colorimetric method of Lanzetta et al. (*27*). The activity inhibited by thapsigargin was considered to be specific SERCA ATPase.

Phosphoenzyme formation with ATP was obtained in reaction mixtures containing 20 mM MOPS, pH 7.0, 80 mM KCl, 1 mM $MgCl_2$, 20 μM $CaCl_2$, 30 μg of microsomal protein/mL, and 5 μM (γ-^{32}P)ATP (ice cold). Following 10 s incubation in ice, the reaction was quenched with perchloric acid (1 M final concentration). Phosphoenzyme formation with P_i was obtained in reaction mixtures containing 25 mM MES, pH 6.2, 5 mM Mg Cl_2, 2 mM EGTA, 20% Me_2SO_4, 0.2 mM (^{32}P)P_i, and 30 μg of microsomal protein/mL. Following 10 min incubation at 30 °C, the reaction was quenched with (ice cold) perchloric acid (1 M final concentration). In all cases BSA (100 μg) was added to each phosphoenzyme sample as a carrier protein, and the samples were washed by centrifugation and resuspension with 0.125 M perchloric acid (twice), and once with cold water. The final sediments were solubilized with 2% lithium dodecyl sulfate (1%), MES (10 mM), pH 6.2, glycerol (50%), and bromophenol blue (0.025%). The samples were then subjected to electrophoretic separation (*28*) on 7.5% gels, and the phosphoenzyme was detected by phosphoimaging. In all experiments, the concentration of microsomal protein was corrected to reflect the same ATPase protein concentration, based on Western blot analysis.

Experiments on limited proteolytic digestion of ATPase with proteinase K were performed in media containing 50 mM MOPS, pH 7.0, 50 mM NaCl, 5 mM $MgCl_2$, 2 mM EGTA, 2.1 mM $CaCl_2$, 1.2 mg of microsomal protein, and 0.04 mg of proteinase K/mL. When indicated, AMP-PCP (1 mM), or $AlCl_3$ (50 μM) and NaF (2 mM) were added 30 min before starting the reaction. The concentration of recombinant ATPase was adjusted to the same level in all the experiments on the basis of ATPase estimates obtained from Western blots, and compensated with empty microsomes. The reaction was allowed to proceed at 25 °C and quenched at serial times by the addition of trichloroacetic acid to yield a final 2.5% concentration. The quenched protein was then solubilized by adding sodium dodecyl

Table 1: Listing of SERCA1 Headpiece Mutations Produced for This Study and Their Functional Consequences[a]

domain	sample	ATPase	EP(ATP)	EP(P_i)	Prot(N)	Prot(Al)
	WT	1.0	1.0	1.0	1.0	1.0
N	D426A	0.39	0.40	0.63	0	1.0
N	E486A	0.40	0.38	0.52	0	1.0
N	F487A	0.23	0.05	0.71	0	1.0
N	R489A	0	0.40	0.34	3.0	0.9
N	R560A	0.2	0.03	0.71	0	1.0
N	D601N	0	0.18	0.07	0.2	0.9
P	D351N	0	0.03	0.03	1.2	0
P	D351A	0	0	0	5.0	0
P	K352A	0	0.09	0.04	0	0.5
P	T353A	0.35	0.25	0.19	0.3	0.5
P	T625A	0.22	0.06	0.02	0.2	0.1
P	G626A	0.17	0.03	0.03	0.2	1.0
P	D627N	0.30	0.12	0.05	0.2	1.0
P	D627A	0.25	0.34	0.08	0	1.0
P	K684A	0	0.03	0.03	0	0.5
P	D703A	0.10	0.08	0.12	0	0.3
P	N706A	0	0.51	0.45	4.0	1.0
P	D707A	0	0.25	0.13	0.3	0
A	R134A	0.65	0.40	0.55	0	1.0
A	R139A	0.97	0.44	0.57	1.0	1.0
A	T171A	0.50	0.71	0.90	0.9	1.0
A	R174A	0.60	0.74	0.47	1.3	1.0
A	T181A	0.23	0.40	0.11	0.1	0
A	G182A	0.09	0.59	0.06	0.2	0
A	E183Q	0	0.80	0.80	1.2	1.0

[a] The headpiece domains and the mutated amino acids are listed in the first and second columns, and the residual ATPase activity (ATPase), phosphoenzyme levels obtained with ATP (EP(ATP)) or P_i (EP(P_i)), and protection by nucleotide (prot(N)) and by fluoroaluminate (prot(Al)) are given in the following columns in fractional values as compared to values obtained with WT protein. The overall standard deviation varied between ±0.03 and ±0.20. Several amino acids were mutated previously: T181, G182 and E183 (*37*); D351 and K352 (*18*); T353, G627, and D627 (*40*); F487A and R489A (*41*); R560A (*22*, *42*); D601N, T625A, D703, N706, and D707 (*43*); K684, D703, and D707 (*44*). For a recent review, see Wuytack et al. (*45*).

sulfate (1%), Tris (0.312 M), pH 6.8, sucrose (3.75%), β-mercaptoethanol (1.25 mM), and bromophenol blue (0.025%). The samples were then subjected to electrophoretic separation (*29*) on 12.5% gels followed by staining with Coomassie Blue or Western blotting. For this purpose, the monoclonal antibody mAb CaF3-5C3 to the chicken SERCA-1 protein and goat anti-mouse IgG-horseradish peroxidase-conjugated secondary antibodies were used, followed by densitometry of the bands visualized with an enhanced chemiluminescence-linked detection system (Amersham Bioscience).

RESULTS

Twenty-five amino acid residues were subjected to site directed mutagenesis within the "N", "P", and "A" domains of the ATPase (Table 1). Expression of recombinant protein was obtained from COS1 cells infected with adenovirus vectors that carried WT or mutated cDNA encoding the ATPase under control of the CMV promoter. Electrophoretic analysis of microsomes obtained from infected cells shows a prominent ATPase band (Figure 2). No corresponding band was observed in microsomes obtained from cells infected with empty vectors. The high content of recombinant ATPase allowed measurements of ATPase activity and partial reactions using the native microsomal preparation, with no need for purification and reconstitution in artificial proteoliposomes. Mutant protein was expressed at levels equal to, or 10−40% below, the levels of WT protein, but in all cases sufficient for the experimentation described below. Microsomes derived from infected cells sustained Ca^{2+} dependent and thapsigargin sensitive ATPase activity (Figure 3A). For each specific sample, the activity was related to the ATPase expression level revealed by Western blots, with reference to a WT sample. We also measured steady state levels of phosphoenzyme obtained by utilization of ATP in the presence of Ca^{2+}, as well as equilibrium levels of phosphoenzyme obtained by reaction with P_i in the absence of Ca^{2+}. Finally, we evaluated whether nucleotide or fluoroaluminate binding protected the ATPase from digestion by proteinase K (*30*). For this purpose, we used an inactive ATP analogue (AMP-PCP) that produces the conformational effect of nucleotide binding without being utilized for the phosphoryl transfer reaction. We also studied protection from proteinase K upon fluoroaluminate binding, which yields a stable analogue of the phosphoenzyme intermediate E1P (*31*). We reasoned that nucleotide or fluoroaluminate binding in the presence of Ca^{2+} would yield conformational states that correspond to important steps for ATPase activation and energy transduction, i.e., substrate induced conformational fit (*32*) and Ca^{2+} occlusion following phosphorylation (*13*).

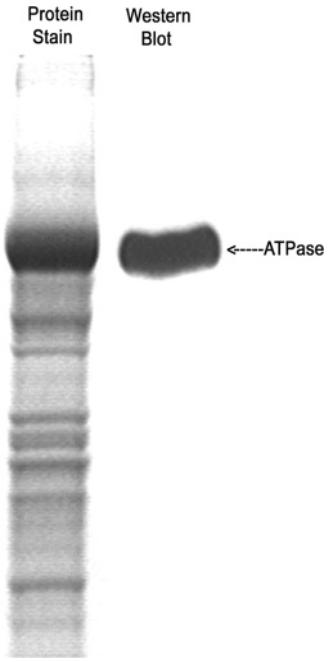

FIGURE 2: Electrophoretic analysis of the protein components of microsomes derived from COS-1 cells infected with adenovirus vectors for expression of exogenous (WT) SERCA-1 protein. The lane on the left side was subjected to protein staining with Coomassie Blue. The lane on the right was subjected to Western blotting for immunodetection of SERCA-1 with monoclonal antibodies. See Materials and Methods for techniques of infections, microsome preparation, and electrophoresis analysis.

The proteinase K digestion sites (Lys119 and Thr242) reside in the loop connecting the "A" domain to transmembrane segments M2 and M3, respectively, and their protection reflects "A"-domain tilting produced by nucleotide binding and/or phosphoenzyme formation by ATP. It should be pointed out that incubation of WT enzyme with proteinase K produces ATPase inactivation, which is prevented by AMP-PCP or fluoroaluminate in parallel with protection from

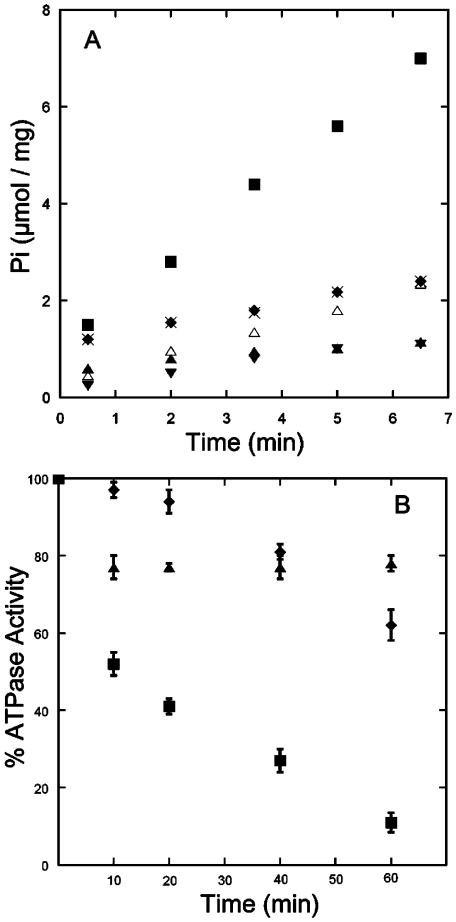

FIGURE 3: ATPase activity of WT and mutant ATPase. Ca^{2+} dependent and TG sensitive ATPase was measured as described in Materials and Methods. (A) The activities of WT (■), Phe487Ala (◆), Asp351Ala (▼), Arg489Ala (△), Gly625Ala (×) and Glu183Gln (▲) mutants is given in the figures. A complete list of ATPase activities for all the mutants is given in Table 1. (B) Inactivation of WT ATPase by digestion with proteinase K in the absence (■) or in the presence of 1 mM AMP-PCP (◆) or 0.1 mM fluoroaluminate (▲). Digestion with proteinase K was performed as described in Materials and Methods, and at various time intervals small volumes were diluted in a reaction mixture for determination of ATPase activity.

proteolytic digestion (Figure 3B). In the mutants with low or no ATPase activity, the protective effect of AMP-PCP and fluoroaluminate was clearly documented by following the pattern of proteolytic digestion.

"N" Domain Residues. The "N" domain has been identified as the nucleotide binding domain (*3*, *16*, *17*, *19*−*22*). In fact, we found that mutation of Phe487 or Arg560 to Ala produces nearly complete inhibition of ATPase activity and phosphoenzyme formation with ATP (Table 1; Figures 3 and 4A). Furthermore, nucleotide protection of ATPase digestion from proteinase K was not observed (Figure 4B), indicating that these single mutations interfere with nucleotide binding. On the other hand, only a minor reduction of phosphoenzyme formed by utilization of P_i (Figure 4A), and normal protection from proteinase K digestion were observed in the presence of fluoroaluminate (Figure 4B). Structural analysis of E1-AMP-PCP indicates (Figure 5) that Phe487 is involved in ring stacking with adenine, and the Arg560 side chain interacts with the β-phosphate of ATP, in addition to forming a salt bridge with Asp627 ("P" domain). This salt bridge is not formed in $E2{\cdot}MgF_4^{2-}$. Our experiments indicate that

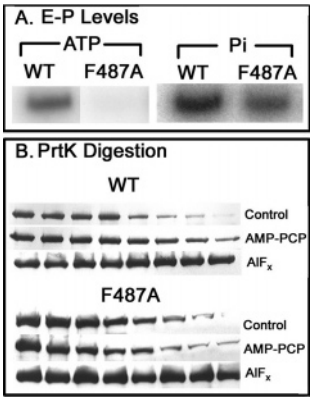

FIGURE 4: Comparative features of WT and Phe487Ala mutant SERCA-1 proteins. (A) Phosphoenzyme (E-P) obtained with ATP in the presence of Ca^{2+}. (B) Proteinase digestion pattern (0, 5, 10, 20, 40, 60, 80, and 120 min, corresponding to the electrophoretic gels from left to right) in the absence or in the presence of AMP-PCP or fluoroaluminate. Experimental conditions are described in Materials and Methods.

these interactions are essential for nucleotide binding, but do not have a major influence on the reactivity of the P domain to P_i, consistent with the crystal structure.

Mutation of Asp426 to Ala produces 60% inhibition of ATPase activity and phosphoenzyme formation with ATP, and 40% inhibition of phosphoenzyme formation with P_i (Table 1). Protection from proteinase K by nucleotide is much reduced, while protection by fluoroaluminate is normal (Table 1). Structural analysis shows interaction of Asp426 with two Arg in the A domain (the Arg134 side chain and the Arg139 main chain amide) in the $E1{\cdot}AlF_x{\cdot}ADP$ crystals, with consequent stabilization of the N and A domains in the E1P state. Interference with this stabilization may explain the effect of the Asp426 mutation.

Mutation of Glu486 to Ala produces 60% inhibition of ATPase activity and phosphoenzyme formation with ATP or P_i (Table 1). No nucleotide protection from proteinase K was observed with this mutant, while protection by AlF_x remained normal. The effect of this mutation is likely due to interference with the hydrogen bond between Glu486 and the Thr171 side chain, and with the consequent stabilization of "N" and "A" domains in the E1P and E2P states. It is noteworthy that the Glu486 partner is different (i.e., His190) in the E2 state, and this may play a role in enzyme isomerization during the catalytic cycle.

The Arg489 to Ala mutant retains no ATPase activity, and much reduced formation of phosphoenzyme from ATP or P_i (Table 1 and Figure 6A). On the other hand, protection from proteinase K is high with nucleotide, and normal with fluoroaluminate (Figure 6B). Analysis of the E1·AMP-PCP structure suggests that the Arg489 side chain coordinates the nucleotide α-phosphate and may position the phosphate chain favorably for utilization of γ-phosphate. On the other hand, Arg489 is at the interface of the "N" and "A" domains, and is important for forming the right interface between them. Replacement of Arg489 with Ala will prevent salt bridge formations in the E2 state with Gln202 and Asp203 in the A domain, therefore interfering with intramolecular stabilization that favors phosphoenzyme formation with P_i. While these stabilization effects are required for the catalytic reactions, they are not evidently necessary and may in fact favor binding of nucleotide in a position that causes "A"-

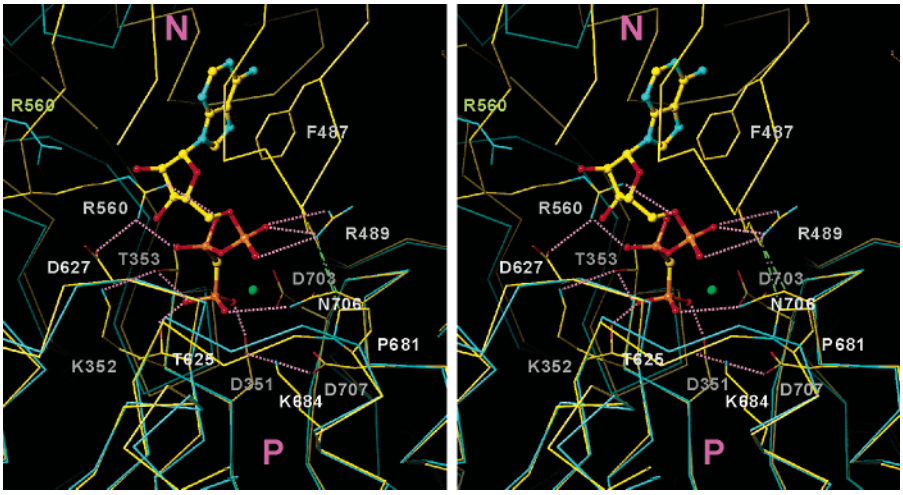

FIGURE 5: A stereoview of the N domain−P domain interface in the E1·AMP-PCP crystal structure (PDB accession code 1VFP). Also superimposed is (cyan) the C-alpha trace of E2·MgF42 (PBD accession code 1WPG) with Arg560 side chain (green label). AMP-PCP is shown in ball-and-stick. Mg^{2+} appears as a small green sphere. Also shown are some of the likely hydrogen bonds (pink dotted lines) and van der Waals contacts of Arg489 (green dashed−dotted lines). Some of the N domain of the E1·AMP-PCP structure is removed for clarity, as well as the A domain of the $E2{\cdot}MgF_4^{2-}$.

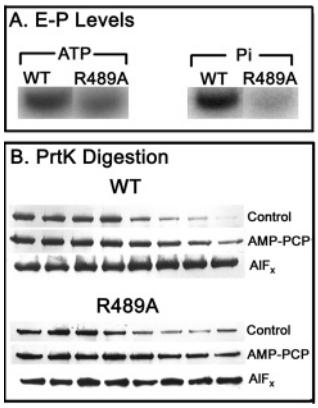

FIGURE 6: Comparative features of WT and Arg489Ala mutant SERCA-1 proteins. (A) Phosphoenzyme (E-P) obtained with ATP in the presence of Ca^{2+}. (B) Proteinase digestion pattern (0, 5, 10, 20, 40, 60, 80, and 120 min, corresponding to the electrophoretic gels from left to right) in the absence or in the presence of AMP-PCP or fluoroaluminate. Experimental conditions are described in Materials and Methods.

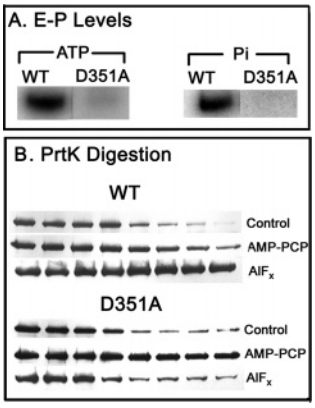

FIGURE 7: Comparative features of WT and Asp351Ala mutant SERCA-1 proteins. (A) Phosphoenzyme (E-P) obtained with ATP in the presence of Ca^{2+}. (B) Proteinase digestion pattern (0, 5, 10, 20, 40, 60, 80, and 120 min, corresponding to the electrophoretic gels from left to right) in the absence or in the presence of AMP-PCP or fluoroaluminate. Experimental conditions are described in Materials and Methods.

domain tilting by P-domain distortion and effective protection from proteinase K digestion. Arg489 in the E1·AMP-PCP and $E1{\cdot}AlF_x{\cdot}ADP$ crystals makes van der Waals contacts with Pro681 and Asn706 side chains in the P domain, apparently to keep the right distance between the two domains. This could be a very important interaction because both Pro681 and Asn706 are absolutely conserved in all P-type ATPases. It is likely that a tighter binding of nucleotide γ-phosphate is allowed if Arg489 is replaced by a smaller residue. In fact, the Asn706Ala mutation also causes a larger protection from proteinase K digestion. The P-domain distortion is expected to be maximal with AlF_x alone, and not affected by these mutations.

The Asp601 to Asn mutant retains no ATPase activity, no phosphoenzyme formation from ATP or P_i, and no nucleotide protection from proteinase K, while protection by fluoroaluminate remains nearly normal (Table 1). Asp601 is located in the hinge region, and is likely to contribute to the relative positioning of N and P domains. Within the hinge region, it makes hydrogen bonds with the Asn359 amide, and the Thr357 side chain to make the hinge region β-strand like (*4*, *33*), so that accurate orientation of the N-domain movement is possible. Evidently these interactions are very important to domain positioning, substrate interactions, and catalytic chemistry. This mutation also substantiates the idea that the N domain is not necessary for the A-domain tilting, unless fluoroaluminate oriented the N domain correctly.

"P" Domain Residues. Mutation of Asp351 to Asn eliminates completely ATPase activity (Table 1), phosphoenzyme formation from ATP or P_i, and protection from proteinase K by fluoroaluminate (Figure 7A,B). This is due to the primary role of Asp351 as the acceptor in the phosphorylation reaction forming a covalent intermediate in the catalytic cycle (*14*, *15*). It is interesting, however, that protection from proteinase K by nucleotide is still observed, and is actually greater with the Asp351Asn mutant, and much greater when Asp351 is mutated to Ala (Figure 7B). This indicates that the nucleotide substrate still binds to the mutants, but phosphoryl transfer does not occur. The greater protection observed with the Ala mutant suggests electrostatic

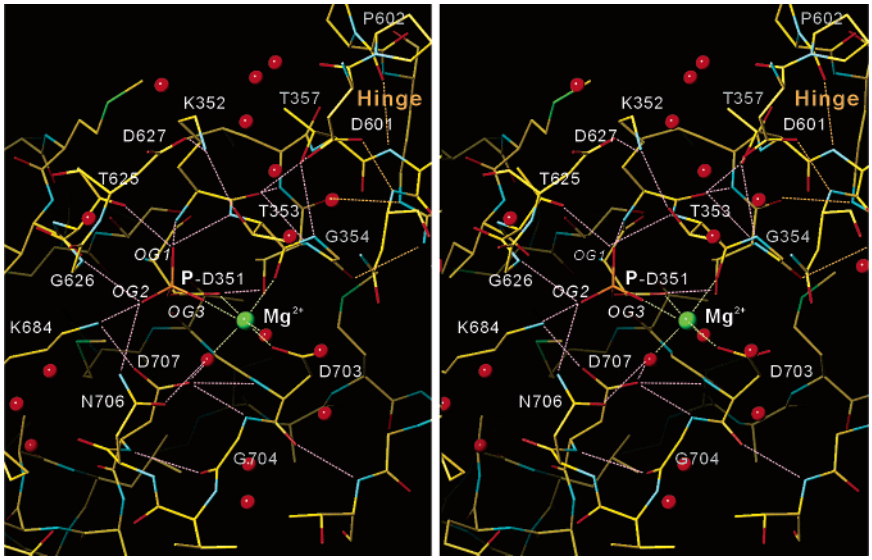

FIGURE 8: Stereoview of the phosphorylation site. Derived from the structure of E2·MgF_4^{2-} (*6*), with aspartylphosphate taken from CheY (PDB accession code 1QMP (*36*)). The small green sphere represents Mg^{2+}, and the red spheres represent water. Coordinations of Mg^{2+} are indicated with broken lines in green; likely hydrogen bonds are shown in pink (not exhaustive). OG1−OG3 refer to the oxygen atoms in the aspartylphosphate. The atomic model of the aspartylphosphate was taken from the related protein CheY (PDB accession code 1QMP), a bacterial response regulator, superimposed with the main chain of Asp351 without changing the side chain conformation (*6*).

repulsion of the nucleotide γ-phosphate by Asp351, whereby the nucleotide phosphate chain acquires prevalently a folded configuration in the WT enzyme (*34*), but a prevalently extended configuration in the Asp351Ala mutant. It is noteworthy that phosphoryl transfer does not occur when AMP-PCP (rather that ATP) is the substrate, even if the WT Asp351 is present. In this case the lack of phosphoryl transfer is related to a different electron distribution and the bond angle of the terminal phosphate with carbon.

Mutation of Lys352 to Ala eliminates completely ATPase activity, phosphoenzyme formation with ATP or P_i, and protection from proteinase K by nucleotide (Table 1). Significant protection by fluoroaluminate, however, is still observed. This residue is highly conserved in the P-type ATPase family but not in other members of the haloacid dehalogenase superfamily (*23*); in many of them it is Leu or Met. It is Phe in the PSPase with no apparent functional role (*24*). Lys352 is coordinated with Thr353 as well as Asp627 in the E1·AMP-PCP and E2·MgF_4^{2-} structures (see below for role of Thr353), but not coordinated directly with substrates. This is in marked contrast with Lys684, but the effects of mutations listed in Table 1 are very much the same. As described previously (*5*) the P domain is distorted by the binding of γ-phosphate (or its analogues). This distortion brings the loops containing Thr353 and Asp627 closer (about 1.0 Å for Cα). These two residues and Thr625 are expected to be critical for guiding the γ-phosphate in the correct position, and will be separated by repulsion unless mediated by Lys352 (Figure 8). It is also conceivable that long side chain is effective in excluding water from the vicinity of Asp351. The inhibition produced by the Lys352 mutation demonstrates that these interactions are crucial to enzyme phosphorylation and the progress of the catalytic cycle. On the other hand, the Lys352 main chain amide is coordinated to a fluoroaluminate fluorine atom (but not to any of the AMP-PCP oxygen atoms). This main chain amide interaction is retained following mutation, and therefore formation of the fluoroaluminate phosphoenzyme analogue is not interfered with.

Mutation of Thr353 to Ala reduces by approximately 70% ATPase activity, phosphoenzyme formation from ATP or P_i, and protection from proteinase K by nucleotide (Table 1). It also reduces protection by fluoroaluminate by approximately 50%. As described in the previous paragraph, Thr353 hydroxyl is hydrogen bonded to γ-phosphate or its analogues. Its main chain position is important for the coordination of Mg^{2+} with its main chain carbonyl oxygen, whereas its side chain position is affected by Lys352. These strategic roles of Thr353 readily explain the mutational results.

Thr625-Gly626-Asp627 constitutes a highly conserved motif in P-type ATPases. In particular, Thr625 is very well conserved in all the haloacid dehalogenase superfamily, although it is on some occasions substituted with Ser. Gly626 is also well conserved, but Asp627 is specific to P-type ATPases. In fact, mutation of Thr625 to Ala produces nearly complete inhibition of ATPase activity and phosphoenzyme formation with ATP or P_i (Table 1 and Figures 2 and 9A). Furthermore, protection from proteinase K by nucleotide, as well as by fluoroaluminate, is interfered with (Figure 9B). Thr625 is on the opposite side of the γ-phosphate to Thr353 and is expected to have similar functional roles. In the phosphate-bound forms, its position appears to be affected by Asp627, which is in turn linked to Thr353 by Lys352. Although Thr353 is linked to Asp351 by coordination to Mg^{2+}, no such strong positioning mechanism is present for the TGD loop. Then it is understandable that the mutational effects are similar to Thr353 but more stringent. These mutations are not deleterious, because they simply remove one of the stabilizing factors; in the case of Lys352, they destroy multiple factors and completely abolish the ATPase activity.

Mutation of Gly626 to Ala interferes strongly with ATPase activity, with phosphoenzyme formation with ATP or P_i, and with protection from proteinase K by nucleotide, while

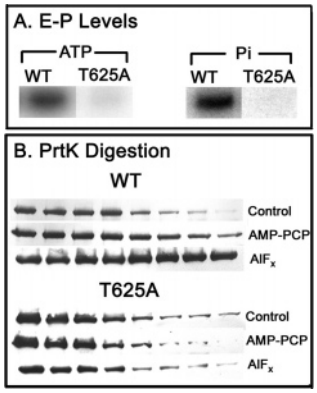

FIGURE 9: Comparative features of WT and Gly625Ala mutant SERCA-1 proteins. (A) Phosphoenzyme (E-P) obtained with ATP in the presence of Ca^{2+}. (B) Proteinase digestion pattern (0, 5, 10, 20, 40, 60, 80, and 120 min, corresponding to the electrophoretic gels from left to right) in the absence or in the presence of AMP-PCP or fluoroaluminate. Experimental conditions are described in Materials and Methods.

protection by AlF_x remains equal to that observed with WT enzyme (Table 1). Structural analysis indicates that the Gly626 main chain amide interacts with a phosphate oxygen atom. However, this phosphate oxygen is stabilized also by Lys684 and Asn706. Therefore, the protection by AlF_x remains to be normal. The Gly626Ala mutant strongly interferes with the binding of nucleotide, because the Ala side chain makes steric collisions with α and β phosphates, thus resulting in interference with ATP−Mg binding. In the $E2{\cdot}MgF_4^{2-}$ form, the Gly626Ala mutant will cause steric collisions with Thr181, preventing proper domain closure.

Mutation of Asp627 to Asn or Ala produces approximately 70% inhibition of ATPase activity, phosphoenzyme formation with ATP or P_i, and protection from proteinase K by nucleotide. Protection by fluoroaluminate remains at normal levels. Structural analysis suggests that this residue has dual roles. Upon nucleotide binding to the WT enzyme, approximation of the N and P domains allows a salt bridge to be formed between Asp627 and Arg560. This would result in cooperative stabilization of the two domains through interaction of the Arg560 guanido group with the ATP β-phosphate and Asp627. Presumably the interaction of Asp627 with Arg560 is weakened following ADP dissociation, and this allows relative displacement of the N and P domains. The other role is, as described earlier, to link the ^{625}TGD loop to the ^{351}DKTGT loop by a salt bridge with Lys352 for forming a proper phosphate binding site. For these reasons, protection from proteinase K (i.e., ATP binding), as well as enzyme phosphorylation with ATP and P_i, is interfered with by mutation of Asp627.

Lys684 is very well conserved in all the members of the haloacid dehalogenase superfamily. What is critical is the position of the side chain nitrogen that stabilizes the γ-phosphate and Asp351. In some of the members (e.g., phosphoglucomutase), the position of this residue is offset by one residue, but the position of the nitrogen is exactly the same. Mutation of Lys684 to Ala produces total inhibition of ATPase activity, phosphoenzyme formation with ATP or P_i, and protection from proteinase K by nucleotide (Table 1). Protection by fluoroaluminate is also interfered with, significantly. It is evident that stabilization of phosphate oxygen by the Lys684 side chain is very important.

Mutation of Asp703, a very well conserved residue through all the members of the haloacid dehalogenase superfamily, to Ala interferes strongly with ATPase activity, phosphoenzyme formation with ATP or P_i, and protection from proteinase K by nucleotide or fluoroaluminate (Table 1). The Asp703 side chain participates in coordination of Mg^{2+}, which is also coordinated by oxygen atoms from the Asp351 side chain, the phosphate substrate, and the Thr353 main chain carbonyl. Evidently, these interactions are of crucial importance to intermediate catalytic reactions.

Mutation of Asn706 to Ala produces total inhibition of ATPase activity, but only 50% reduction of the phosphoenzyme levels obtained with ATP or P_i. On the other hand, protection from proteinase K by nucleotide is higher than observed with the WT enzyme, and protection by AlF_x is normal (Table 1). This residue is absolutely conserved in P-type ATPases and appears to have multiple functional roles. Asn706 provides stabilization of γ-phosphate itself and a very important water molecule which is coordinated to Mg^{2+}. The functional consequences of Asn706 mutation suggest that, in the absence of stabilization by Asn706, phosphorylation of Asp351 is permitted to some extent, but subsequent processing of the phosphoenzyme through the catalytic cycle is impaired. In addition to interference of water and Mg^{2+} coordination, the Asn706Ala mutation may allow Lys684 to come closer to the ATP γ-phosphate, thereby acquiring a position yielding greater protection from proteinase K. This is because, as noted for Arg489, Asn706 makes van der Waals contacts with Lys684 apparently to keep an appropriate distance between the N and P domains. In $E2{\cdot}MgF_4^{2-}$ crystals, Asn706 interacts with Thr181 presumably to keep the right distance between the A and P domains. Inappropriate domain interactions caused by Asn706Ala mutation may explain the total suppression of ATPase activity while keeping the phosphorylation levels reasonably high.

Mutation of Asp707 to Ala produces total inhibition of ATPase activity, and strong reduction of phosphoenzyme formation with ATP or P_i, and of protection from proteinase K by nucleotide or fluoroaluminate (Table 1). It is clear that Asp707 stabilizes Lys684 by side chain interaction, and may also contribute in orienting the Asp351 side chain. In addition, it is likely to sustain hydrogen bonding with Asp703 and Gln704 amides throughout the reaction cycle to stabilize the ^{702}GDG loop. The functional consequences of Asp707 mutation demonstrate that the conformational and positional role of this residue is crucial to all binding and catalytic reactions of the ATPase cycle.

A Domain Residues. Mutation of Arg134 reduces the ATPase activity by 35%, inhibits phosphoenzyme formation with ATP by 60%, and inhibits phosphoenzyme formation with P_i by 45%. It interferes with protection from proteinase K by nucleotide, but not by fluoroaluminate (Table 1). As suggested above, interaction of the Arg134 side chain with Asp426 is likely to provide stabilization of "N" and "A" domains in the $E1{\cdot}ATP$ state. Furthermore, positioning of Asp426 by Arg134 may be important for ATP binding (see effect of Asp426, above). Interference with these interactions may explain the effects of the Arg134 mutation. On the contrary, mutation of Arg139 does not produce significant inhibition of ATPase activity or nucleotide protection from proteinase K, since it is its main chain amide that provides

further stabilization of the "N" and "A" domains through interaction with Asp426. This interaction would be retained following mutation of the side chain.

Mutation of Thr171 to Ala produces approximately 50% inhibition of ATPase activity, 30% inhibition of phosphoenzyme formation with ATP, and no significant inhibition of phosphoenzyme obtained with P_i. Protection from proteinase K by nucleotide or fluoroaluminate remains at normal levels (Table 1). Thr171 interacts with Glu486, providing a nearly unique link between the "N" and "A" domains in E1·AMP-PCP and E1·AlF_x·ADP. The functional consequences of Thr171 mutation suggest weakening of this interaction, thereby producing a less favorable environment for phosphoenzyme formation. We have seen above that mutation of Glu486 is more damaging inasmuch as Glu486 switches partner and interacts with His190 in the E2 state and therefore provides conformational stability as domain interactions change through the entire cycle.

Mutation of Arg174 to Ala produces approximately 40% reduction of ATPase activity, 25% inhibition of phosphoenzyme formation with ATP, and 50% inhibition of phosphoenzyme formation with P_i. Protection from proteinase K by ATP or P_i remains at normal levels (Table 1). This residue is at the A/N interface. In E2, it interacts with Asp422 in the N domain through a water molecule. In E2·MgF_4^{2-}, it makes a hydrogen bond with Phe487 amide through a water and van der Waals contacts with the Phe487 side chain, thus interfering with the phosphorylation reaction.

Thr181, Gly182, and Glu183 are highly conserved and form a part of a hairpin structure, which is maintained by a hydrogen bond between Thr181 hydroxyl and Glu183 amide. The main chain dihedral angle is allowed for Gly but unfavorable for others. Mutation of these residues produces total or strong inhibition of ATPase activity. The levels of phosphoenzyme obtained with ATP are reduced in the Thr181 and Gln182 mutants, while phosphoenzyme formation with P_i and protection by nucleotide or fluoroaluminate from proteinase K digestion are strongly interfered with (Table 1). Thr181Ala and Gly182Ala mutants will destroy the hairpin structure and might affect the entire conformation of the A domain. Otherwise total inhibition of protection by AlF_x is not readily explained, because this loop is located outside of the A domain and has no interactions with other parts in E1·AlF_x·ADP. Phosphorylation with P_i is nearly completely lost with the Gly182Ala mutant. This is because the Cβ atom of Ala causes steric conflicts with the bound phosphate.

On the other hand, the Glu183Gln mutant retains normal formation of phosphoenzyme with ATP or P_i, and normal protection by nucleotide or fluoroaluminate from proteinase K remains strong (Figure 10), in spite of total ATPase inhibition (Table 1 and Figure 3). The extraordinary specificity of the functional effect of the Glu183 mutation is due to the role of Glu183 in positioning of a water molecule that is required for hydrolytic cleavage of E2P (*35*). Thus, the last step of the ATPase reaction cycle, that is, dephosphorylation of the acylphosphate, is totally suppressed with this mutant.

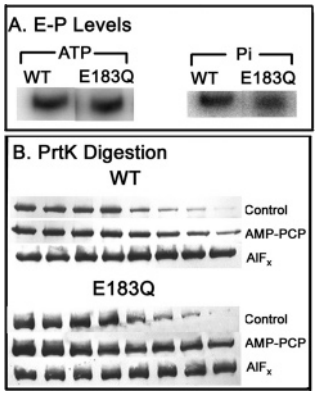

FIGURE 10: Comparative features of WT and Glu183Gln mutant SERCA-1 proteins. (A) Phosphoenzyme (E-P) obtained with ATP in the presence of Ca^{2+}. (B) Proteinase digestion pattern (0, 5, 10, 20, 40, 60, 80, and 120 min, corresponding to the electrophoretic gels from left to right) in the absence or in the presence of AMP-PCP or fluoroaluminate. Experimental conditions are described in Materials and Methods.

DISCUSSION

We selected for our analysis several headpiece amino acids that either are highly conserved in the P-type ATPase family, or are positioned in seemingly critical sites of the enzyme structure, or were previously singled out by studies of protein chemistry and mutagenesis. Within the N domain, our functional analysis demonstrates unambiguously that Phe487 and Arg560 are required for ATP binding through ring stacking with adenine, and interaction with the β-phosphate of ATP, respectively. In addition, Arg560 forms a salt bridge with Asp627, thereby contributing to "N" and "P" domain cross-linking (Figure 5). It is remarkable that mutation of either of these residues interferes strongly with ATP binding and utilization, while having only a small effect on the "P" domain reactivity to P_i (Figure 4A and Table 1). The functional involvement of Phe487, Arg560, and Asp627 highlights the importance of interdomain interactions in promoting phosphoryl transfer from ATP.

Interference with ATP binding, as revealed by reduced nucleotide protection from proteinase K, is also produced by mutations of other N domain residues such as Glu486 (next to Phe487), Asp426, and Asp601. An exception is Arg489, whose mutation apparently does not interfere with nucleotide binding and actually increases protection from proteinase K (Figure 6). It is possible that interaction of Arg489 with the nucleotide α-phosphate keeps ATP in a position that is not optimal for the protective effect. Arg489 mutation (in analogy to the Asn706 and Asp351 mutations as explained below) may then allow phosphate chain extension and closer interaction of γ-phosphate with Lys684, thereby affording greater protection. On the other hand, Arg489 appears to have a conformational role in virtue of its hydrogen bonding with the Gln202 and Asp203 (E2 state). Interference with proper stabilization of the N and A domains, as well as with coordination of the nucleotide α-phosphate, is likely to be responsible for the catalytic inhibition produced by the Arg489 mutation.

Glu486 and Asp601 have positional roles, as they contribute to stabilization of the three domains in various states. Glu486 is likely to interact with the Thr171 side chain to stabilize "N" and "A" domains in the E1P and E2P states, while switching to His190 in the E2 state. On the other hand Asp601, within the hinge region, contributes to orienting the N domain with respect to the P domain through interactions with the Asn359 backbone amide, with the Thr357 side

Table 2: Interactions of Amino Acid Residues Subjected to Mutational Analysis[a]

residue		interaction	states	function
Asp426	N	Arg134; Arg139 carbonyl	E1·ATP−E1P	N/A interface
Glu486	N	Thr171	E1·ATP−E2·P_i	N/A interface
		His190	E2	N/A interface
Phe487	N	ATP (adenine ring)	E1·ATP	ATP binding
Arg489	N	Gln202; Asp203; van der Waals contact with Val200	E2	N/A interface
		ATP (α-PO_4); van der Waals contact with Pro681 and Asn706	E1·ATP	ATP binding
		van der Waals contacts with Ile188 and His190	E2·P_i	N/A interface
Arg560	N	ATP (β-PO_4)	E1·ATP	ATP binding
		Asp627	E1·ATP−E1P	N/P interface
Asp601	N	Thr357; Asn359 amide	all	N/P (hinge)
		Lys352	E1P	positioning
		Lys352 (via water)	E1, E2	
Asp351	P	ATP (γ-PO_4) or P_i; Mg^{2+}	E1·ATP−E2·P_i	covalent reaction
Lys352	P	Thr353	E1−E2·P_i	positioning
		Asp627	E1·ATP−E2·P_i	positioning
		Asp601 (via water)	E1, E2	positioning
Thr353	P	ATP (γ-PO_4) or P_i	E1·ATP−E2·P_i	phosphate
		Lys352	E2·P_i	positioning
		carbonyl−Mg^{2+}	E1·ATP−E2·P_i	Mg^{2+}
		Glu183	E2·P_i	A/P interface
Thr625	P	ATP (γ-PO_4) or P_i	E1·ATP−E2·P_i	phosphate
Gly626	P	amide−ATP (γ-PO4) or P_i	E1·ATP−E2·P_i	ATP binding
Asp627	P	Arg560	E1·ATP−E1P	N/P interface
		Lys352	E1·ATP−E2·P_i	positioning
Lys684	P	ATP (γ-PO_4) or P_i		phosphate
		Asp351, Asp707	all	positioning
		Asn706	E1·ATP−E2·P_i	positioning
Asp703	P	Mg^{2+}	E1·ATP−E2·P_i	Mg^{2+}
Asn706	P	ATP (γ-PO4) or P_i	E1·ATP−E2·P_i	phosphate
		H_2O coordinating Mg^{2+}		Mg^{2+}
		Lys684 (repulsion)		positioning
		van der Waals contact with Arg489	E1·ATP−E1P	N/P interface
		Thr181 carbonyl; van der Waals contact with Gly182	E2·P_i	A/P interface
Asp707	P	Asp703 amide; Gly704 amide	all	conformational
		Asp351 (repulsion? or H-bond?)	E1·ATP−E2·P_i	positioning
		Lys684	E1·ATP−E2·P_i	positioning
Arg134	A	Asp426	E1·ATP−E1P	A/N interface
Thr171	A	Glu486	E1P−E2·P_i	A/N interface
Arg174	A	Phe487 amide; also van der Waals contacts with Phe487	E2·P_i	A/N interface
		Asp422 through a water	E2	A/N interface
Thr181	A	Glu183 amide	all	conformational ?
		carbonyl-Asn706	E2·P_i	A/P interface
Gly182	A	allows Thr181−Glu183 interaction	all	conformational
		van der Waals contact with Asn706	E2·P_i	A/P interface
		water coordinating Mg^{2+} (amide)		Mg^{2+}
Glu183	A	water attacking phosphate	E2P ↔ E2+P_i	positioning of water
		Thr353	E2·P_i	A/P interface
		phosphate	E2·P_i	phosphate

[a] N/P and N/A signify stabilization of domain interface in a specific enzyme state, as indicated.

chain, and possibly with Lys352. Evidently these interactions are very important to domain movement and substrate positioning, as well as catalytic chemistry. The Asp601 residue is highly conserved within the P-type ATPase family.

All the "P" domain residues studied by us are highly conserved, and their mutation interferes with ATP binding and all catalytic reactions. Two exceptions to nucleotide binding interference are mutations of Asp351 (especially to Ala) and of Asn706, inasmuch as they increase markedly (rather than interfere with) the protection from proteinase K by nucleotide (Table 1, Figure 7). It is likely that, in the WT enzyme, repulsion between γ-phosphate and Asp351, as well as Asn706 interaction with Arg489 in the N domain, positions bound nucleotide in a less than optimal position for the protective effect. Mutational removal of such constraints would then allow the ATP to acquire a more effective position through a closer interaction with Lys684. In spite of retaining nucleotide binding, the Asp351 mutants manifest total loss of all catalytic reactions, due to the role of Asp351 as the direct acceptor of phosphate.

Mutation effects of the residues in the P domain can be explained quantitatively to some extent. As illustrated in Figure 8, which is deduced from the structure of E2·MgF_4^{2-} and aspartylphosphate taken from CheY (PDB accession code 1QMP (*36*)), the three oxygen atoms of γ-phosphate are in quite different environments. OG1 is coordinated by Thr353 amide, Lys352 amide, and Thr625 hydroxyl. Thr353 hydroxyl is not as close as Thr625 hydroxyl (3.7 vs 2.9 Å) to OG1, although close to the corresponding atom in AMP-PCP (2.5 Å). OG2 is coordinated by Gly626 amide, and Lys684 and Asn706 side chain. OG3 is stabilized essentially by Mg^{2+} alone. As noted earlier, Lys352 must be critical in positioning the ^{625}TGD loop; its amide position will be affected by its side chain interaction with Thr353 and Asp627. Thus, Lys352Ala mutant is likely deleterious due to its 3-fold roles. Thr353Ala mutation is thus expected to

be less effective than Thr625Ala in phosphorylation but similar in AMP-PCP protection from proteinase K digestion.

Also within the "P" domain, Asp703, Asn706, and Asp707 play crucial roles. The Asp703 side chain participates in coordination of Mg^{2+}, which is also coordinated by oxygen atoms from the Asp351 side chain, the phosphate substrate, and the Thr353 main chain. Asn706 coordinates the γ-phosphate (OG2) and a water molecule, which, in turn, is coordinated to Mg^{2+} thereby providing stabilization of the phosphate$-Mg^{2+}$ complex. Finally, Asp707 stabilizes K684, which is, in turn, involved in interaction with a phosphate oxygen atom.

Within the "A" domain, we subjected Arg134, Arg139, Thr171, and Arg174 to mutational analysis. Although these residues were not highly conserved, we were interested in them for their positions at the interface of the "A" domain with the "N" domain. Interaction of the Arg134 side chain with Asp426 is likely to provide stabilization of "N" and "A" domains in the E1-ATP state, which is augmented by interaction of the Arg139 main chain amide with Asp426. On the other hand, stabilization of the "A" and "N" domains in the E1P state is likely to be provided by interaction of Thr171 with Glu486, linking the "N" and "A" domains. We noted above that mutation of Glu486 switches partner from Thr171 to His190 in the E2 state. We find that mutation of these residues (with the exception of Arg139) produces significant inhibition of ATPase kinetics. We attribute this effect to interference with the role of these residues in optimizing the positional stability of the "A" domain in specific states corresponding to intermediate reaction of the catalytic cycle. Thr181, Gln 182, and Glu183, still in the "A" domain, are highly conserved, and their mutation produces strong inhibition of ATPase activity.

Previous studies (*37*) indicated that mutation of any of these three residues interferes with the E1P ↔ E2P transition, while a more recent and specific study of Glu183 (*34*) indicated that mutation of this residue interferes with hydrolytic cleavage of E2P.

We find that the steady state phosphoenzyme level formed with ATP is reduced, while phosphoenzyme formation with P_i and nucleotide or fluoroaluminate protection from proteinase K digestion are strongly interfered with by the Thr181 and Gly182 mutations. On the other hand, we find that mutation of Glu183 allows a normal level of phosphoenzyme obtained with ATP or P_i, as well as normal nucleotide and fluoroaluminate protection from proteinase K (Table 1 and Figure 10), even though the ATPase hydrolytic activity is totally inhibited.

The Thr181, Gly182, and Glu183 residues reside on the A domain outer surface in E1P, but at the A/P interface in E2P, and are involved in a hydrogen bonding network including water molecules, substrate, and P domain residues (*6*). Our experiments indicate that Thr181 and Gly182 play an important structural role in forming a hairpin structure. On the other hand, Glu183 appears to have a more specific role in stabilization of a water molecule, which is required for the final hydrolytic cleavage of E2P.

We finally note that formation of a stable phosphoenzyme analogue with fluoroaluminate is not interfered with by any of our mutations in the N domain. Rather, strong interference is produced by mutation of Asp351, Thr625, Lys684, and Asp707. This interference is related to the role of Asp351 as the direct acceptor, interaction of fluorine atoms with the Thr625 and Lys684 side chains, and stabilization of Lys684 by Asp707 for this purpose. As compared with phosphoenzyme formation with P_i, participation of Lys352, Thr353, and Asp703 appears to be less stringently required, and Asn706 does not play a significant role in formation of the fluoroaluminate analogue. This suggests that stabilization of Mg^{2+} by these residues is in fact more important for electrophilic assistance in the phosphorylation reaction than for stabilization of the fluoroaluminate complex. The absence of mutation effects of the residues in the N domain on the protection by AlF_x suggests that the A-domain tilting that causes protection from proteinase K digestion does not require the contribution of the N domain.

In conclusion, combined mutational and structural analysis identifies and demonstrates the functional roles of interactions that are directly involved in binding nucleotide (such as Phe487 and Arg560 in the N domain) and phosphate substrate (such as Asp351, Thr625, Lys684, and Thr353 in the P domain). Furthermore, several amino acids are identified whose role may be defined as positional, inasmuch as they are involved in stabilizing neighboring residues for optimal substrate or Mg^{2+} binding, or stabilizing the relative positions of headpiece domains as they change with the progress of sequential catalytic reactions (Table 2). Cross-linking of "N" and "P" domains upon ATP binding, as well as rotation and tilting of the "A" domain in the E1·ATP, E1P, and E2P transitions, is involved in triggering displacements of transmembrane segments. In fact, sequential establishment and disruption of domain−domain interactions is a major device in the long-range linkage of catalytic and Ca^{2+} binding functions. The sequence of specific arrangements is driven by substrate binding, phosphorylation, and dissociation of products, and by related changes of interdomain spacing and "P" domain distortion. In turn, the "P" domain is anchored by hydrogen bonding to the transmembrane domain directly or through the L6/7 loop, where site directed mutations (e.g., Lys819Ala and Arg822Ala) were found (*38*) to interfere with catalytic reactions.

REFERENCES

1. de Meis, L., and Vianna, A. L. (1979) Energy interconversion by the Ca^{2+}-dependent ATPase of the sarcoplasmic reticulum, *Annu. Rev. Biochem. 48*, 275−292.
2. MacLennan, D. H., Brandl, C. J., Korczak, B., and Green, N. M. (1985) Amino-acid sequence of a Ca^{2+} + Mg^{2+}-dependent ATPase from rabbit muscle sarcoplasmic reticulum, deduced from its complementary DNA sequence, *Nature 316*, 696−700.
3. Toyoshima, C., Nakasako, M., Nomura, and Ogawa, H. (2000) Crystal structure of the calcium pump of sarcoplasmic reticulum at 2.6 Å resolution, *Nature 405*, 647−655.
4. Toyoshima, C., and Nomura, H. (2002) Structural changes in the calcium pump accompanying the dissociation of calcium, *Nature 418*, 605−611.
5. Toyoshima, C., and Mizutani, T. (2004) Crystal structure of the calcium pump with a bound ATP analogue, *Nature 430*, 529−535.
6. Toyoshima, C., Nomura, H., and Tsuda, T. (2004) Lumenal gating mechanism revealed in calcium pump crystal structures with phosphate analogues, *Nature 432*, 361−368.
7. Sørensen, T. L., Møller, J. V., and Nissen, P. (2004) Phosphoryl transfer and calcium ion occlusion in the calcium pump, *Science 304*, 1672−1675.
8. Chen, B., Squier, T. C., and Bigelow, D. J. (2004) Calcium activation of the Ca-ATPase enhances conformational heterogeneity between nucleotide binding and phosphorylation domains, *Biochemistry 43*, 4366−4374.

9. Clarke, D. M., Loo, T. W., Inesi, G., and MacLennan, D. H. (1989) Location of high affinity Ca^{2+}-binding sites within the predicted transmembrane domain of the sarcoplasmic reticulum Ca^{2+}-ATPase. *Nature 339*, 476−478.
10. Andersen, J. P., and Vilsen, B. (1992) Functional consequences of alterations to Glu309, Glu771, and Asp800 in the Ca^{2+}-ATPase of sarcoplasmic reticulum, *J. Biol. Chem*. *267*, 19383−19387.
11. Zhang, Z., Lewis, D., Strock, C., Inesi, G., Nakasako, M., Nomura, H., and Toyoshima, C. (2000) Detailed characterization of the cooperative mechanism of Ca^{2+} binding and catalytic activation in the Ca^{2+} transport (SERCA) ATPase, *Biochemistry 39*, 8758−8767.
12. Vilsen, B., and Andersen, J. P. (1998) Mutation to the glutamate in the fourth membrane segment of Na+,K+-ATPase and Ca^{2+}-ATPase affects cation binding from both sides of the membrane and destabilizes the occluded enzyme forms, *Biochemistry 37*, 10961−10971.
13. Inesi, G., Ma, H., Lewis, D., and Xu, C. (2004) Ca^{2+} occlusion and gating function of Glu309 in the ADP-fluoroaluminate analog of the Ca^{2+}-ATPase phosphoenzyme intermediate, *J. Biol. Chem*. *279*, 31629−31637.
14. Degani, and Boyer, P. D. (1973) A borohydride reduction method for characterization of the acyl phosphate linkage in proteins and its application to sarcoplasmic reticulum adenosine triphosphatase. *J. Biol. Chem*. *248*, 8222−8226.
15. Bastide, F., Meissner, G., Fleischer, S., and Post, R. L. (1973) Similarity of the active site of phosphorylation of the adenosine triphosphatase from transport of sodium and potassium ions in kidney to that for transport of calcium ions in the sarcoplasmic reticulum of muscle, *J. Biol. Chem. 248*, 8385−8391.
16. Murphy, A. J. (1977) Sarcoplasmic reticulum adenosine triphosphatase: labeling of an essential lysyl residue with pyridoxal-5′-phosphate, *Arch. Biochem. Biophys. 180*, 114−120.
17. Mitchinson, C., Wilderspin, A. F., Trinnaman, B. J., and Green, N. M. (1982) Identification of labelled peptide after stoicheiometric reaction of fluorescein isothiocyanate with the Ca^{2+}-dependent adenosine triphosphatase of sarcoplasmic reticulum, *FEBS Lett. 146*, 87−92.
18. Maruyama, K., and MacLennan, D. H. (1988) Mutation of aspartic acid-351, lysine-352, and lysine-515 alters the Ca^{2+} transport activity of the Ca^{2+}-ATPase expressed in COS-1 cells, *Proc. Natl. Acad. Sci. U.S.A 85*, 3314−3318.
19. McIntosh, D. B., Woolley, D. G., and Berman, M. C. (1992) 2′,3′-O-(2,4,6-trinitrophenyl)-8-azido-AMP and -ATP photolabel Lys-492 at the active site of sarcoplasmic reticulum Ca($^{2+}$)-ATPase, *J. Biol. Chem. 267*, 5301−5309.
20. Yamagata, K., Daiho, T., and Kanazawa, T. (1993) Labeling of lysine 492 with pyridoxal 5′-phosphate in the sarcoplasmic reticulum Ca^{2+}-ATPase. Lysine 492 residue is located outside the fluorescein 5-isothiocyanate-binding region in or near the ATP binding site, *J. Biol. Chem. 268*, 20930−20936.
21. Andersen, J. P. (1995) Dissection of the functional domains of the sarcoplasmic reticulum Ca^{2+}-ATPase by site-directed mutagenesis, *Biosci. Rep. 15*, 243−261.
22. Hua, S., Ma, H., Lewis, D., Inesi, G., and Toyoshima, C. (2002) Functional role of "N" (nucleotide) and "P" (phosphorylation) domain interactions in the sarcoplasmic reticulum (SERCA) ATPase, *Biochemistry 41*, 2264−2272.
23. Aravind, L., Galperin, M. Y., and Koonin, E. V. (1998) The catalytic domain of the P-type ATPase has the haloacid dehalogenase fold, *Trends Biochem. Sci. 23*, 127−129.
24. Wang, W., Cho, H. S., Kim, R., Jancarik, J., Yokota, H., Nguyen, H. H., Grigoriev, I. V., Wemmer, D. E., and Kim, S. H. (2002) Structural characterization of the reaction pathway in phosphoserine phosphatase: crystallographic "snapshots" of intermediate states, *J. Mol. Biol. 319*, 421−431.
25. Karin, N. J., Kaprielian, Z., and Fambrough, D. M. (1989) Expression of avian Ca^{2+}-ATPase in cultured mouse myogenic cells, *Mol. Cell Biol. 9*, 1978−1986.
26. Zhang, Z., Lewis, D., Strock, C., Inesi, G., Nakasako, M., Nomura, H., and Toyoshima, C. (2000) Detailed characterization of the cooperative mechanism of Ca^{2+} binding and catalytic activation in the Ca($^{2+}$) transport (SERCA) ATPase, *Biochemistry 39*, 8758−8767.
27. Lanzetta, P. A., Alvarez, L. J., Reinach, P. S., and Candia, O. A. (1979) An improved assay for nanomole amounts of inorganic phosphate, *Anal. Biochem. 100*, 95−97.
28. Weber, K., and Osborn, M. (1969) The reliability of molecular weight determinations by dodecyl sulfate-polyacrylamide gel electrophoresis, *J. Biol. Chem. 244*, 4406−4412.
29. Laemmli, U. K. (1970) Cleavage of structural proteins during the assembly of the head of bacteriophage T4, *Nature 227*, 680−685.
30. Danko, S., Yamasaki, K., Daiho, T., Suzuki, H., and Toyoshima, C. (2001) Organization of cytoplasmic domains of sarcoplasmic reticulum Ca^{2+}-ATPase in E_1P and E_1ATP states: a limited proteolysis study, *FEBS Lett. 505*, 129−135.
31. Troullier, A., Girardet, J. L., and Dupont, Y. (1992) Fluoroaluminate complexes are bifunctional analogues of phosphate in sarcoplasmic reticulum Ca^{2+}-ATPase, *J. Biol. Chem. 267*, 22821−22829.
32. Ma. H, Inesi, G., and Toyoshima, C. (2003) Substrate-induced Conformational Fit and Headpiece Closure in the Ca^{2+} ATPase (SERCA), *J. Biol. Chem. 278*, 28938−28943.
33. Hayward, S. (1999) Structural principles governing domain motions in proteins, *Proteins 36*, 425−435.
34. Hua, S., Inesi, G., Nomura, H., and Toyoshima, C. (2002) Fe^{2+}-catalyzed oxidation and cleavage of sarcoplasmic reticulum ATPase reveals Mg^{2+} and Mg^{2+}-ATP sites, *Biochemistry 41*, 11405−11410.
35. Clausen, J. D., Vilsen, B., McIntosh, D. B., Einholm, A. P., and Andersen, J. P. (2004) Glutamate-183 in the conserved TGES motif of domain A of sarcoplasmic reticulum Ca^{2+}-ATPase assists in catalysis of E2/E2P partial reactions, *Proc. Natl. Acad. Sci. U.S.A 101*, 2776−2781.
36. Lewis, R. J., Brannigan, J. A., Muchova, K., Barak, I., and Wilkinson, A. J. (1999) Phosphorylated aspartate in the structure of a response regulator protein, *J. Mol. Biol. 294*, 9−15.
37. Clarke, D. M., Loo, T. W., and MacLennan, D. H. (1990) Functional consequences of alterations to am ino acids located in the nucleotide binding domain of the Ca^{2+}-ATPase of sarcoplasmic reticulum, *J. Biol. Chem. 265*, 22223−22227.
38. Zhang, Z., Lewis, D., Sumbilla, C., Inesi, G., and Toyoshima, C. (2001) The role of the M6-M7 loop (L67) in stabilization of the phosphorylation and Ca^{2+} binding domains of the sarcoplasmic reticulum Ca^{2+}-ATPase (SERCA), *J. Biol. Chem. 276*, 15232−15239.
39. Kraulis, P. J. (1991) MOLSCRIPT: a program to produce both detailed and schematic plots of protein structures. *J. Appl. Crystallogr. 24*, 946−950.
40. Maruyama, K., Clarke, D. M., Fujii, J., Inesi, G., Loo, T. W., and MacLennan, D. H. (1989) Functional consequences of alterations to amino acids located in the catalytic center (isoleucine 348 to threonine 357) and nucleotide-binding domain of the Ca^{2+}-ATPase of sarcoplasmic reticulum, *J. Biol. Chem. 264*, 13038−13042.
41. McIntosh, D. B., Woolley, D. G., Vilsen, B., and Andersen, J. P. (1996) Mutagenesis of segment ^{487}Phe-Ser-Arg-Asp-Arg-Lys^{492} of sarcoplasmic reticulum Ca^{2+}-ATPase produces pumps defective in ATP binding, *J. Biol. Chem. 271*, 25778−25789.
42. Clausen, J. D., McIntosh, D. B., Vilsen, B., Woolley, D. C., and Andersen, J. P. (2003) Importance of N-domain residues T441, Glu442, Lys515, Arg560, and Leu562 of sarcoplasmic reticulum Ca^{2+}-ATPase for MgATP binding and subsequent catalytic steps. Plasticity of the nucleotide-binding site, *J. Biol. Chem. 278*, 20245−20258.
43. Clarke, D. M., Loo, T. W., and MacLennan, D. H. (1990) Functional consequences of mutations of conserved amino acids in the beta-strand domain of the Ca^{2+}-ATPase of sarcoplasmic reticulum, *J. Biol. Chem. 265*, 14088−14092.
44. Vilsen, B., Andersen, J. P., and MacLennan, D. H. (1991) Functional consequences of alterations to amino acids located in the hinge domain of the Ca^{2+}-ATPase of sarcoplasmic reticulum, *J. Biol. Chem. 266*, 16157−16164.
45. Wuytack, F., Raeymaekers, L., and Missiaen, L. (2002) Molecular physiology of the SERCA and SPCA pumps, *Cell Calcium 32*, 279−305.

BI050332M